



CrossMark  
click for updates

Cite this: *RSC Adv.*, 2016, 6, 15143

## The effect of protein concentration on the viscosity of a recombinant albumin solution formulation†

Andrea D. Gonçalves,‡<sup>a</sup> Cameron Alexander,<sup>a</sup> Clive J. Roberts,<sup>a</sup> Sebastian G. Spain,§<sup>a</sup> Shahid Uddin<sup>b</sup> and Stephanie Allen\*<sup>a</sup>

The effect of protein concentration on solution viscosity in a commercially available biopharmaceutical formulation of recombinant albumin (rAlbumin) was studied. The level of protein aggregation with concentration and its impact on solution viscosity was investigated. Theoretical models predicting viscosity with concentration were applied to these data, and a model that accounts for multiple protein species in solution provided the best fit. The results highlight the need to account for heterogeneity in the level of aggregation when addressing the increase of viscosity observed at high concentrations of protein solutions, a significant issue for the manufacture and use of protein-based therapeutics.

Received 11th October 2015  
Accepted 28th January 2016

DOI: 10.1039/c5ra21068b

www.rsc.org/advances

### Introduction

The viscosity of protein formulations is an important issue for the biopharmaceutical industry due to its practical implications in medicine manufacture and administration.<sup>1</sup> Biopharmaceutical liquid formulations are frequently created with high protein concentrations, due to the need for high mass delivery to overcome low potency. Low volumes are also desirable to allow patient self-administration in cost effective devices.<sup>1,2</sup> However, when biomacromolecules reach high solution concentrations, problems such as high viscosity and poor flow properties, as well as stability issues, can occur.

Theories from colloidal science have been used to model the observed increases in solution viscosities with increased macromolecular content.<sup>3–5</sup> A number of these are based on approximations to hard spherical repulsive particles, and have been applied with some success.<sup>6,7</sup> However, there are more molecular properties, such as shape,<sup>8</sup> charge distribution<sup>9,10</sup> or kinetics of association,<sup>11–13</sup> which need to be considered for more accurate predictions of protein solution viscosity. Moreover, such properties depend on factors including pH, temperature, ionic strength and the presence of additives in solution, and therefore these and their impact on the formation of higher order oligomeric biomolecular species and/or aggregates need also to be considered.

The effect of protein concentration on solution viscosity has been discussed previously.<sup>10,14–19</sup> At dilute concentrations, protein solution viscosity has been studied using models that account for the hydrodynamic behaviour of proteins in a fluid.<sup>15</sup> Other theories that account for inter-protein interaction potential and excluded volume have been applied with relative success in predicting the increase of viscosity with protein concentration.<sup>4,7</sup> In general, all these models assume that (globular) proteins are hard spherical or quasi-spherical macromolecules and, to some extent, are able to explain the increase of viscosity with concentration and allow a comparison with the behaviour of colloidal dispersions. So far, however, there has not been a theoretical model that is capable of predicting the viscosity of protein solutions in a range from dilute to highly concentrated (>200 mg mL<sup>-1</sup>).

Intrinsic viscosity ( $[\eta]$ ) is a hydrodynamic parameter that is related to the conformation and size of a molecule in dilute solution and represents the effective molecular volume at these conditions.<sup>20</sup> It is defined in terms of concentration ( $c$ , in mg mL<sup>-1</sup>) by the following equation:

$$[\eta] = \lim_{c \rightarrow 0} \left( \frac{\eta - \eta_0}{c} \right) \quad (1)$$

where  $\eta$  is the solution viscosity and  $\eta_0$  is the viscosity of the solvent. One of the hard (quasi)-spherical models relating protein viscosity and concentration, is the modified Mooney equation<sup>21</sup> as per Ross-Minton's approach,<sup>18</sup> defined by:

$$\eta_{\text{rel}} = \frac{\eta}{\eta_0} = e^{\left[ \frac{[\eta]c}{1 - \frac{\kappa}{\nu} [\eta]c} \right]} \quad (2)$$

where relative viscosity ( $\eta/\eta_0$ ) is an exponential function of concentration ( $c$ ),  $[\eta]$ , a crowding effect factor ( $\kappa$ ) and Simha's shape factor ( $\nu$ ).<sup>15</sup> As the crowding effect is a consequence of the excluded volume when the protein concentration increases, the

<sup>a</sup>School of Pharmacy, The University of Nottingham, University Park, Nottingham, NG7 2RD, UK. E-mail: stephanie.allen@nottingham.ac.uk

<sup>b</sup>Formulation Sciences, MedImmune, LLC, Cambridge, CB21 6GH, UK

† Electronic supplementary information (ESI) available. See DOI: 10.1039/c5ra21068b

‡ Current address: Particle Sciences, Devices and Engineering, R & D, GSK, Medicines Research Centre, Stevenage, SG1 2NY, UK.

§ Current address: Department of Chemistry, University of Sheffield, Dainton Building, Sheffield, S3 7HF, UK.

model predicts solution viscosity accounting for the protein's shape and its excluded volume.

From colloidal rheology, the Krieger–Dougherty model (eqn (3)),<sup>3</sup>

$$\eta_{\text{rel}} = \frac{\eta}{\eta_0} = \left(1 - \frac{\phi}{\phi_{\text{max}}}\right)^{-\phi_{\text{max}}[\eta]} \quad (3)$$

was originally applied to describe infinite dilutions of hard spherical particles. In the case of random close packing of spheres at low deformations,<sup>4,22</sup> the intrinsic viscosity ( $[\eta]$ ) in eqn (3) is fixed to 2.5 and is dimensionless, since it is defined as a function of volume fraction ( $\phi$ ), with a maximum packing fraction ( $\phi_{\text{max}}$ ) of 0.64. Still assuming the spherical shape, this maximum packing fraction has been discussed to be around 0.71, when the particles are exposed to higher shear rates.<sup>4</sup>

The Russel–Saville–Schowalter revision of Batchelor's equation<sup>4</sup> (eqn (4)), is a model which predicts the increase of viscosity of hard spherical particles, while taking into account interparticle interactions based on the effective distance between particles.

$$\eta_{\text{rel}} = \frac{\eta}{\eta_0} = 1 + 2.5\phi + s\phi^2 + O(\phi^3) \quad (4)$$

where the coefficient  $s$  of the quadratic term is defined by,

$$s = 2.5 + \frac{3}{40} \left(\frac{d_{\text{eff}}}{a}\right)^5 \quad (5)$$

and is dependent on the effective interparticle distance,  $d_{\text{eff}}$ , and the radius of particle,  $a$ . The factor  $d_{\text{eff}}$  is dependent on both the hydrodynamic contributions of the particle as well as the interaction potential, relevant to the dispersion conditions. Batchelor showed that for a concentrated dispersion of hard spherical repulsive particles, the value of  $s$  is equal to 6.2, where  $d_{\text{eff}} = 2a$ .<sup>4</sup>

The models described above assume that any change in composition of protein species in solution is negligible. Parameters in these models typically account for only one species of a specific shape and size. Some authors have addressed the problem for binary mixtures of different sized particles, to predict the impact of this on the solution viscosity.<sup>5,23–25</sup> In recent reports, binary blends of proteins have been studied by controlling the content of each protein in solution and understanding the effect of this on the overall solution viscosity.<sup>14,26</sup>

Galush *et al.*<sup>26</sup> presented a study on the viscosity of mixed protein solutions, using mixtures of different monoclonal antibodies (mAbs) and of one mAb with BSA. Their conclusions derived from measuring the viscosity of both the individual protein solutions and blends. They proposed that the viscosity of protein blends could be predicted by an additive function of the viscosity of each individual protein multiplied by its respective known weight fraction (eqn (6)).

$$\ln \eta(w_{\text{tot}}, f_2) = (1 - f_2) \ln \eta_1(w_{\text{tot}}) + f_2 \ln \eta_2(w_{\text{tot}}) \quad (6)$$

where  $\eta_1$  and  $\eta_2$  are the viscosities of pure protein 1 and 2, respectively,  $f_1$  and  $f_2$  are the weight fractions corresponding to

the protein 1 and 2 present in the blend and  $w_{\text{tot}}$  is the total weight/volume concentration of the protein mixture.

Minton<sup>14</sup> has contributed with the generalisation of eqn (2) and (3) and application to predicting the viscosity of globular protein solutions containing only one protein, but with relatively well-known fractions of its monomeric and higher order associative species. The generalised models of Ross–Minton (eqn (7)) and Krieger–Dougherty (eqn (8)) models, as proposed by Minton, are as follows:

$$\frac{\eta}{\eta_0} = \exp \left[ \frac{[\eta]_w w_{\text{tot}}}{1 - \frac{w_{\text{tot}}}{w^*}} \right] \quad (7)$$

$$\frac{\eta}{\eta_0} = \left(1 - \frac{w_{\text{tot}}}{w^*}\right)^{-[\eta]_w w^*} \quad (8)$$

Note that the Krieger–Dougherty equation has been modified to allow the use of weight/volume concentrations ( $w_{\text{tot}}$ , in  $[\text{mg mL}^{-1}]$ ), rather than volume fractions. Both eqn (7) and (8) are now represented as functions of  $w_{\text{tot}}$ ,  $[\eta]_w$  and  $w^*$ . The parameter  $[\eta]_w$  is weight-averaged intrinsic viscosity (in  $[\text{mg mL}^{-1}]$ ), described in eqn (9). The parameter  $w^*$  represents an estimated protein concentration above which the solution cannot flow, referred to as jamming concentration.<sup>14,22</sup>

$$[\eta]_w = \sum \frac{w_i [\eta]_i}{w_{\text{tot}}} \quad (9)$$

Here a recombinant human albumin (rAlbumin) solution formulated in a buffer containing salt and a surfactant was studied. The rAlbumin studied is expressed in *Saccharomyces cerevisiae* and has an identical amino acid sequence to human serum albumin (HSA).<sup>27</sup> HSA is the most abundant protein in the blood at a concentration of  $\sim 40 \text{ mg mL}^{-1}$ . It is the major transport protein for unesterified fatty acids, having the capacity to bind numerous metabolites, active pharmaceutical ingredients as well as other organic molecules.<sup>28</sup>

Our study investigated the rheological characteristics of HSA samples with concentrations ranging from  $0.1 \text{ mg mL}^{-1}$  to approximately  $500 \text{ mg mL}^{-1}$ , using steady shear rheology with a torsional rheometer. A detailed biophysical characterisation of these samples was performed to account for the level of aggregation, size and shape of protein species, within higher concentrations of rAlbumin, to probe relationships between aggregation and solution viscosity. The ultimate goal was to predict the viscosity of highly concentrated globular protein solutions, using the abovementioned models to enhance the efficacy of formulated biopharmaceuticals.

## Materials and methods

### Materials

Recombinant human albumin (rAlbumin) was donated by Novozymes Biopharma UK Ltd. (Nottingham, UK) in the form of Recombum® Prime (batches: 1104 and 1101). The product is a liquid formulation of concentration  $200 \text{ mg mL}^{-1}$ , stored at

2–8 °C. All other reagents were obtained from Sigma-Aldrich, UK and were of analytical grade. The formulation buffer of Recombin® Prime is composed of NaCl (145 mM), polysorbate-80 (15 mg L<sup>-1</sup>) and sodium octanoate (32 mM) in ultrapure water (pH = 7.0 ± 0.3 at room temperature). Another buffer was prepared containing only NaCl (145 mM) in ultrapure water (pH = 7.0 ± 0.3).

Centrifugal concentrators (Vivaspin 20 – 5 kDa molecular weight cut-off with polyethersulfone membrane; Sartorius Stedim, Ltd., UK) were used to concentrate rAlbumin samples to higher concentrations than the starting material (200 mg mL<sup>-1</sup>). The procedure recommended by the manufacturer was followed, using a fixed 45° rotor centrifuge (Hermle Z400, Labortechnik GmbH, Germany). After centrifugation, samples were collected, mixed and checked for their concentration using UV-visible spectroscopy. All samples and the respective buffers were stored at 2–8 °C.

## Methods

**Quantification of protein concentration by UV-visible spectroscopy.** An Agilent 8453 UV-vis spectrophotometer (model G1103, Agilent Technologies, Germany) was used to quantify protein concentration *via* absorbance at 280 nm. A quartz cuvette with 1 cm path length (Hellma, Germany) was used for all measurements.

For all protein solutions at concentrations higher than 50 mg mL<sup>-1</sup>, a double dilution scheme was followed to allow a measurement of sample diluted to 0.5 mg mL<sup>-1</sup>. Each second dilution was produced in triplicate so that the absorbance measurement (and posterior concentration calculation) was reported as an average of 3 measurements.

For the determination of concentration of rAlbumin solutions, the percent extinction coefficient at 280 nm ( $A_{1\%}^{1\text{cm}}$ ) used was 5.8.<sup>29</sup>

**Rheology.** The rheometers used were Anton-Paar (Graz, Austria) MCR models 301 and 501. Cone-and-plate geometries used throughout this study were stainless steel CP50-1 (diameter = 50 mm; cone angle = 1°) and CP40-0.3 (diameter = 40 mm; cone angle = 0.3°). To prevent evaporation of sample and to maintain a constant temperature of 20 °C ± 0.1 °C throughout the measurements, an evaporation blocking system equipped with a Peltier unit was used. Prior to measurements, all samples were allowed to equilibrate to room temperature (~23 °C) for at least 40 minutes.

Rotational tests (flow curves and viscosity curves) were performed by controlling the shear rate typically from 0.01 to 1000 s<sup>-1</sup>, and measuring torque, shear viscosity and shear stress. To increase data validity and sensitivity of the method, each shear rate step had a 60 second duration time during which the instrument was averaging over the collected data. Two shear-rate sweeps (ramping down and up) were performed per sample, without waiting time between sweeps. The tests were always started after a 10 minute waiting time after loading the sample.

**Micro-viscometer/rheometer on-a-chip (mVROC).** The mVROC, by Rheosense, Inc. (San Ramon, California, USA) was

used for measurement of air–water interface-free bulk viscosity at high shear rates. The mVROC is a microfluidics slit rheometer where the microfluidics chip is composed of a microchannel (rectangular slit) made of borosilicate glass mounted on a gold-coated silicon base. Viscosity is measured as a function of pressure drop as the fluid flows in the microchannel (width = 3.02 mm; depth depends on the chip used). In a typical experiment, the flow rate,  $Q$ , is varied using a syringe pump and Hamilton gastight glass syringes (Reno, Nevada, USA). The mVROC device outputs the pressure drop as a function of flow rate, which is used to calculate the nominal or apparent viscosity *via*  $\eta(\dot{\gamma}) = \tau_w/\dot{\gamma}_w$ .<sup>30</sup> The true shear rate and true shear viscosities are then calculated, respectively, using the Weissenberg–Rabinowitsch–Mooney equation.<sup>30,31</sup>

Samples analysed were rAlbumin solutions at 200 and 500 mg mL<sup>-1</sup>. For these measurements, the A05 and D05 chips were used and the temperature was kept constant at 20 °C ± 0.1 °C using a water circulation system (ThermoCube, SS cooling systems, USA).

### High performance size exclusion chromatography (HPSEC)

**Determination of level of protein aggregation.** rAlbumin samples were analysed for their level of aggregation using HPSEC. The high performance liquid chromatography (HPLC) system used was from Agilent Technologies 1200 series (Germany) with the following components: degasser, binary pump with a 100 µL injection loop, an autosampler, thermostatted sample tray (at 5 °C), a thermostatted (at room temperature) column holder and a UV detector. The software used for this system was Chemstation for liquid chromatography systems, by Agilent Technologies. A Tosoh Biosciences, LLC (USA), model TSK gel G3000SWxl column was used (7.8 mm (ID) × 30 cm (L)), composed of silica gel particles with mean particle size of 5 µm and pore size of 250 Å. A guard column (silica particles of 7 µm, 6 mm (ID) × 4 cm (L)) was also used with the analytical column.

The mobile phase was an aqueous buffer of 0.1 M sodium sulfate (Na<sub>2</sub>SO<sub>4</sub>) and 0.1 M dibasic sodium phosphate anhydrous (Na<sub>2</sub>HPO<sub>4</sub>), titrated to pH 6.8 with 6 N HCl. This buffer was filtered with 0.22 µm pore size vacuum-driven filter units (PES membrane, EMD Millipore, USA).

All protein samples were diluted to 10 mg mL<sup>-1</sup>, and injection volume was 25 µL. Run time was 20 minutes at a flow rate of 1 mL min<sup>-1</sup>. Each sample was injected three times. Formulation buffers respective to the protein samples were also injected as blanks.

Bio-Rad gel filtration protein standards (Bio-Rad Laboratories, Inc., USA) were used for this method's system suitability test. These were prepared according to the manufacturer's instructions and 25 µL injected once at the beginning and end of 20 sample injections.

All samples, buffers and Bio-Rad protein standards were filtered through 0.45 µm centrifugal filters (Ultrafree-MC PVDF, EMD Millipore, USA). The obtained chromatograms followed integration and peak symmetry and resolution were calculated *via* the method analysis used on the software.

**Analysis with multiple detectors for determination of molecular weight and intrinsic viscosity of rAlbumin solutions.** To calculate bulk molecular weight and intrinsic viscosity, the

chromatography system used was a Polymer Labs GPC 50 Plus (Agilent Technologies, USA) gel permeation unit that comprised an autosampler, a fixed volume injection loop (20  $\mu\text{L}$ ), thermostatted column holder, and the following detectors: a 90° light scattering detector, a refractive index detector, and a differential pressure viscometer. Calibration of the system was made with polyethylene oxide (Polymer Labs, UK) solutions in phosphate buffer saline (Lonza, Inc.).

The method details chosen for these experiments were similar to the previous section with exception that samples were diluted to 15 mg mL<sup>-1</sup>, thus injecting 300  $\mu\text{g}$  of total protein. System suitability was still performed with Bio-Rad protein standards and the same buffer was used as mobile phase. Each rAlbumin sample was injected three times, with buffers injected at least once.  $dn/dc$  used for protein analysis was 0.185 mL g<sup>-1</sup>.<sup>32</sup>

### Dynamic light scattering (DLS)

Sizing measurements were performed using the Zetasizer NanoZS dynamic light scattering instrument (Malvern Instruments, UK). Samples were illuminated by a 633 nm laser and light scattering was detected at 173° by an avalanche photodiode. DLS results were obtained and analysed using the Zetasizer software version 7.01. Protein samples were measured at 1 mg mL<sup>-1</sup> diluted in sample buffer, to reduce non-linearity effects on measurements by increased viscosity of solvent with higher concentrations.

Measurement settings for rAlbumin size readings were at a constant temperature of 20 °C, performing 15 runs of 10 seconds each. An equilibration time of at least 5 minutes was set before the measurement started. Size measurements were made in triplicate with fresh aliquots for each reading.

## Results

### The rheology of formulated recombinant human albumin solutions

The data in Fig. 1A and B show that rAlbumin solutions displayed constant shear viscosities for the increasing shear rates applied (0.01 to 1000 s<sup>-1</sup>). Fig. 1C shows a linear increase of shear stress with the increasing applied shear rates. For the higher concentration materials (400–500 mg mL<sup>-1</sup>) the shear viscosities were from  $\sim 1$  s<sup>-1</sup> onwards, while showing slight non-linear increase of viscosities when  $< 1$  s<sup>-1</sup>. However, in general, throughout the range of concentrations of rAlbumin presented and the applied shear rates, it was considered that these solutions exhibited a Newtonian-like behaviour. Each sample was measured using two consecutive shear rate sweeps, ramping down and up (Fig. 1A and B). Hysteresis effects were not observed, in agreement with the literature, which suggests that the protein molecules diffuse rapidly in the fluid once shear is stopped.<sup>7,33,34</sup>

For comparison between the concentration of samples and the obtained shear viscosities, the viscosity values at 1000 s<sup>-1</sup> were taken from three separate readings per sample and are reported in Fig. 2 as an average with the respective standard deviation. The viscosity values reported here are those at high

shear viscosity ( $\eta_{\infty}$ ), since the viscosities of these samples were overall shear-rate independent.<sup>7</sup> In Fig. 2 the average viscosity values are reported against the average actual concentrations measured for each sample. It was noted that as the targeted protein concentrations were increasingly higher, it was more difficult to achieve such targets (*e.g.*  $\geq 300$  mg mL<sup>-1</sup>; see Table SI-1 from ESI†). For clarity within this manuscript therefore, sample concentrations are referred to as the corresponding target concentration.

From Fig. 2A, the viscosity values were similar for lower protein concentrations. An increase of viscosity with increasing concentration was seen, in agreement to what has been reported throughout the literature with regards to serum albumin solutions.<sup>7,10,15</sup> Most importantly, the exponential trend observed from the data in Fig. 2A is also reported for other globular proteins, such as immunoglobulins.<sup>11–13,35</sup>

### Characterisation of protein species present in recombinant human albumin solutions

Our aim was to correlate the observed increase in viscosities with the level of aggregation present in the increasing concentrations of rAlbumin samples. Therefore, the identification, relative quantification and size characterisation of the monomeric and oligomeric species present in solution was performed using HPSEC, DLS and microfluidic SDS-PAGE (shown in the ESI†).

### High-performance size exclusion chromatography (HPSEC)

HPSEC retention times for the protein species typically present were  $\sim 7.9$ , 8.7 and 9.8 minutes, corresponding to trimer, dimer and monomers, respectively (see Fig. SI-1 from ESI†). This method of analysis produced good resolution between the different identified species and these were comparable to literature values using a similar setup.<sup>36</sup> No higher molecular weight species other than dimers and trimers were found in any of the solutions analysed. This reflected the high purity of the recombinant albumin material due to its manufacturing process generating only a small percentage of trimers and dimers,<sup>27</sup> with the monomer showing the highest relative percentage with a peak area of  $>90\%$ . Samples from 50 to 200 mg mL<sup>-1</sup> had similar peak areas for all protein species. Only when concentrations reached approximately 250 mg mL<sup>-1</sup> and over, a trend could be detected on the increase of dimers and trimers with a corresponding decrease of monomer (Fig. 2B).

Size exclusion chromatography required sample dilution for analysis when concentrations were  $>10$  mg mL<sup>-1</sup>. Dilution is a limitation of this method since it can influence the material's content in relative percentage of each species, as it can be a factor for some aggregates to disassociate, and therefore be considered reversible.<sup>37,38</sup> It was important to understand if this was the case with rAlbumin solutions. By comparing injections of proteins at 50 mg mL<sup>-1</sup> and 10 mg mL<sup>-1</sup> concentrations, their respective peak areas were different by factors of  $<1\%$  (see Fig. SI-2 from ESI†). Such low differences indicated that dissociation upon dilution of trimers and dimers into monomers was negligible. Moreover, this is in agreement with the

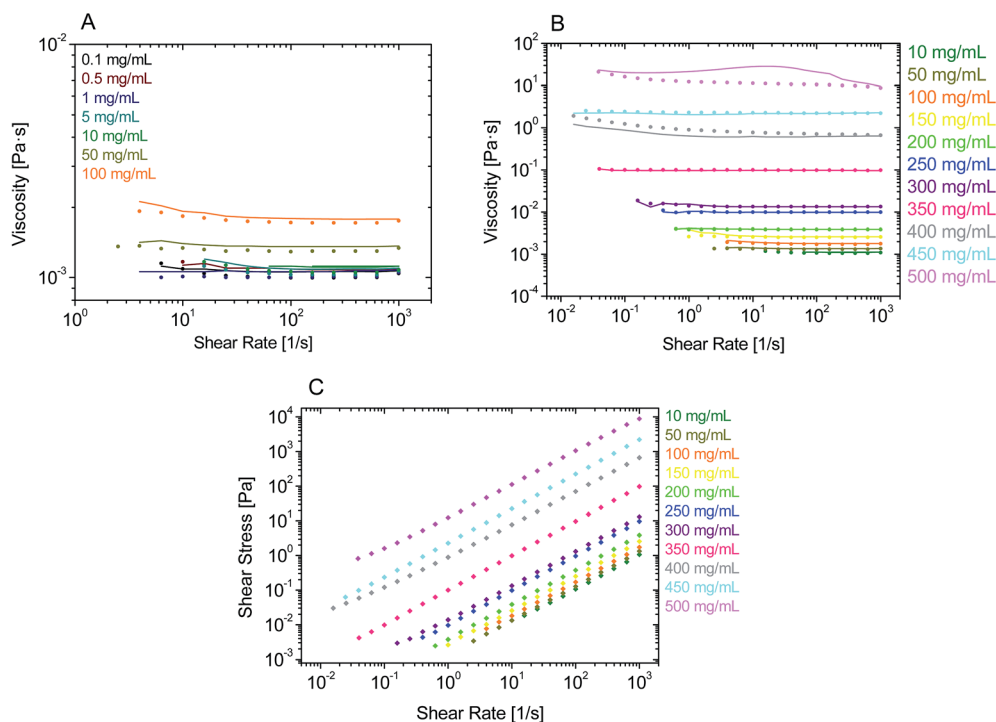


**Fig. 1** Experimental steady shear rheology of rAlbumin solutions obtained with cone–plate 50 mm, 1°, or cone–plate 40 mm, 0.3°, at 20 °C. (A and B) Viscosity values are shown for ramping down (closed circles) and ramping up (lines) shear rates. (A) Samples from 0.1 to 100 mg mL<sup>-1</sup>. (B) Samples from 10 to 500 mg mL<sup>-1</sup>. (C) Flow curves for experimental steady shear rheology of rAlbumin solutions from 10 to 500 mg mL<sup>-1</sup>. Shear stress values are shown only for ramping down shear rates.

irreversibility observed of associated dimer and trimer species reported in prior literature.<sup>39</sup>

Triple-detection HPSEC was used to experimentally determine the intrinsic viscosity and molecular weight (MW) for each of the protein species present in rAlbumin samples: monomer, dimer and trimer. This determination allowed for subsequent analysis discussed ahead in this study.

The results were relative to the two peaks detected corresponding to monomer and dimer, since the differential pressure viscometer could not detect the low percentage of trimers present in solution (see Fig. SI-2 from ESI†). Analysis of peak

areas per sample showed a trend of increasing rAlbumin dimers, similar to what was observed previously for conventional HPSEC (Table 1).

### Dynamic light scattering

The hydrodynamic size analysis of rAlbumin solutions by dynamic light scattering (DLS) was performed for the entire range of solutions after dilution to 1 mg mL<sup>-1</sup>. All solutions were analysed without prior filtration to assess if aggregates were present within the detection limit of DLS (up to 1 μm of

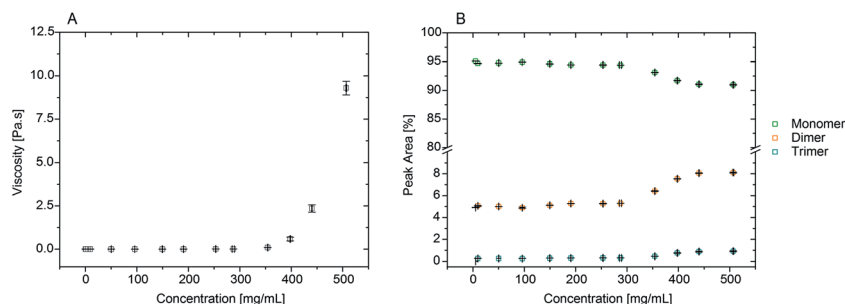


**Fig. 2** (A) Viscosity of rAlbumin solutions ranging from 0.1 mg mL<sup>-1</sup> to 500 mg mL<sup>-1</sup> (target concentrations). Viscosities are taken at high shear ( $\eta = 1000 \text{ s}^{-1}$ ) at 20 °C. Viscosity values are represented as an average and standard deviation (error bars) of 3 separate measurements for each sample. Concentrations are represented as the average of 3 measurements and error bars are standard deviation. (B) HPSEC conventional method for determining level of aggregation of rAlbumin solutions showing relative peak areas in %. Data in squares represent an average of 3 readings per sample. Error bars are standard deviation per sample for peak area% (y-axis) and for concentration (x-axis). All samples were diluted to 10 mg mL<sup>-1</sup> prior to analysis when necessary.

**Table 1** HPSEC triple detection values of peak area, bulk molecular weight (MW) and bulk intrinsic viscosity (IV) for monomers and dimers detected in rAlbumin solutions. Average and standard deviations are reported for 3 separate measurements per sample

Sample (mg mL <sup>-1</sup> )	Monomer			Dimer		
	Peak area (%)	MW (kDa)	[ $\eta$ ] (mL mg <sup>-1</sup> )	Peak area (%)	MW (kDa)	[ $\eta$ ] (mL mg <sup>-1</sup> )
50	96.11 ± 0.03	64 988 ± 297	0.00408 ± 0.00004	3.89 ± 0.02	121 239 ± 1171	0.00482 ± 0.00014
100	95.97 ± 0.10	65 449 ± 933	0.00402 ± 0.00017	4.03 ± 0.10	143 044 ± 12 519	0.00446 ± 0.00089
200	95.71 ± 0.01	64 656 ± 580	0.00408 ± 0.00006	4.29 ± 0.01	130 356 ± 1563	0.00477 ± 0.00044
250	95.68 ± 0.01	64 791 ± 749	0.00409 ± 0.00006	4.32 ± 0.01	132 466 ± 5446	0.00505 ± 0.00072
350	94.69 ± 0.24	66 090 ± 1780	0.00412 ± 0.00005	5.31 ± 0.24	138 341 ± 8136	0.00441 ± 0.00101
400	94.46 ± 0.02	65 290 ± 185	0.00410 ± 0.00003	5.54 ± 0.02	132 674 ± 3686	0.00489 ± 0.00050
450	94.33 ± 0.01	65 358 ± 184	0.00408 ± 0.00004	5.67 ± 0.01	131 680 ± 3886	0.00462 ± 0.00047
500	93.90 ± 0.01	65 066 ± 242	0.00412 ± 0.00006	6.10 ± 0.01	132 140 ± 4754	0.00467 ± 0.00056

hydrodynamic diameter). In all cases, the samples did not show the presence of aggregates. For all the analysed samples, the measured average hydrodynamic radii from the size distributions by intensity ranged between 3.8–4.5 nm corresponding to values reported in literature<sup>40</sup> for a recombinant human albumin solution (Fig. 3). The hydrodynamic size distribution by volume resulted in one peak, with its mean peak value skewed towards lower sizes, closer to the monomer size.

#### Surface tension effects on rheology measurements – control experiments

To ensure that the rheological measurements were taken as accurately as possible and were free of artefacts related to the method and the technical specifications of the rheometer, additional experiments were carried out.

The influence of surface tension at the air–water interface of protein solutions in surfactant-free buffers has been shown to present apparent high-viscosities at low shear rates. The use of a conventional rheometer with cone-and-plate geometry has been suggested as not being the most appropriate instrumentation for these types of samples as it is not an air–water

interface-free technique.<sup>7</sup> Therefore, a rAlbumin solution at 200 mg mL<sup>-1</sup> (from the original formulation) was analysed with the micro viscometer/rheometer-on-a-chip (mVROC) method, which provides rheometry measurements free of air–water interface. When superimposing the cone-and-plate (CP) rheometer data with mVROC data, the sample at 200 mg mL<sup>-1</sup> showed no difference in its viscosity values. As an example, at shear rate  $\approx 1000$  s<sup>-1</sup>, the average viscosities measured with each instrument were  $\eta_{(CP)} \approx 3.5$  mPa s and  $\eta_{(mVROC)} \approx 3.4$  mPa s (Fig. 4). This clearly showed that the rheometer data were most likely free of air–water interfacial artefacts.

In further experiments, samples were prepared by diluting in an aqueous surfactant-free solution of NaCl 145 mM. rAlbumin solutions at 5, 10, 50 and 100 mg mL<sup>-1</sup> were measured on the rheometer and their level of aggregation was assessed by HPSEC and DLS. HPSEC and DLS data were similar to those of formulated rAlbumin. However, while samples at 5, 10 and 50 mg mL<sup>-1</sup> in NaCl 145 mM showed an increase of viscosities towards low shear rates; only the sample at 100 mg mL<sup>-1</sup> of rAlbumin in NaCl 145 mM presented constant viscosities throughout a similar shear rate range (Fig. 5). Samples at 5 and

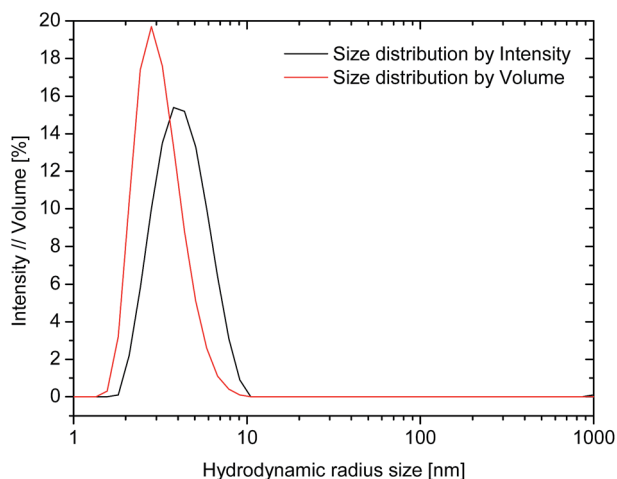


**Fig. 3** Dynamic light scattering plots for 200 mg mL<sup>-1</sup> rAlbumin solution diluted to 1 mg mL<sup>-1</sup>. Size distributions by intensity (black line), and by volume (red line).

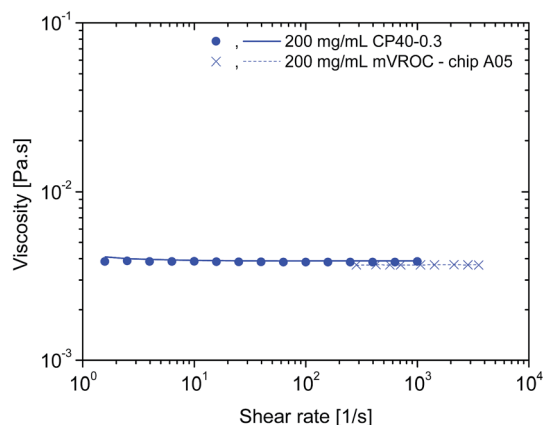


**Fig. 4** mVROC data for 200 mg mL<sup>-1</sup> of rAlbumin in comparison to the cone-and-plate rheology data of the same sample. mVROC data: crosses – ramping up shear rates, dashed lines – ramping down shear rates; CP rheology data: closed circles – ramping up shear rates; lines – ramping down shear rates.

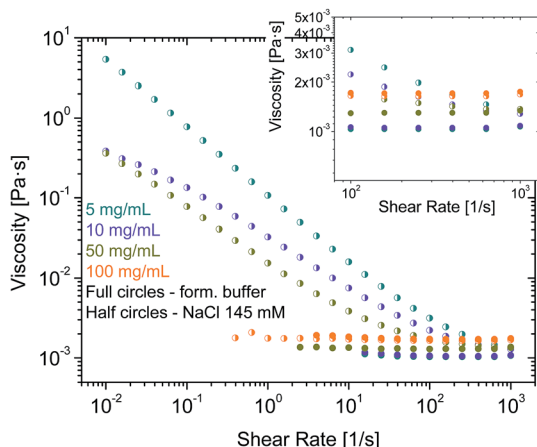


Fig. 5 Viscosity curves for rAlbumin solutions diluted in 145 mM NaCl buffer, in comparison to the material in formulation buffer, at the same concentrations: 5, 10, 50 and 100 mg mL<sup>-1</sup>. Half circles – rAlbumin in 145 mM NaCl only; full circles – rAlbumin in formulation buffer. Inset focuses on the viscosities of these samples at the higher shear rates.

10 mg mL<sup>-1</sup> showed a slightly increased high shear viscosity ( $\eta_{\infty}$  at  $\dot{\gamma} = 1000$  s<sup>-1</sup>), when compared to the data collected from formulated samples.

Additionally, a test was done to assess if the method of concentrating the protein solution would also concentrate the surfactant (see SI-7†). The original sample at 200 mg mL<sup>-1</sup> and the concentrated sample to match 200 mg mL<sup>-1</sup> both presented matching viscosity profiles and values. Therefore, to address the analysis made in this work, the simplest case was considered, where the surfactant would have diffused through the concentrator's membrane during centrifugation for all concentrated samples (>200 mg mL<sup>-1</sup>).

### Effect of high protein concentration on solution viscosity

The intrinsic viscosity of human serum albumin has been reported to be of  $4.73 \times 10^{-3} \pm 1.2 \times 10^{-4}$  mL mg<sup>-1</sup>, for similar solution conditions to these presented here (temperature at 20 °C, pH 7.0).<sup>8</sup> Values of intrinsic viscosity for bovine serum albumin, have been reported to be  $3.7 \times 10^{-3}$  mL mg<sup>-1</sup> (ref. 15) or similar values.<sup>20,41</sup> Although the albumin here used is fatty-acid bound, it is expected that the presence of fatty acid in serum albumin does not influence the value of intrinsic viscosity.<sup>42</sup> Intrinsic viscosity values in literature for HSA<sup>8</sup> and for bovine serum albumin (BSA)<sup>15</sup> were used to fit the rheometry data (Fig. 6) using Ross–Minton's hard (quasi)-spherical equations relating protein viscosity and concentration (eqn (2)).

Our rheology data was fitted to eqn (2), with the intrinsic viscosity ( $[\eta]$ ) constrained and the  $\kappa/\nu$  factor freely floating (Fig. 6 – blue and orange line). The computed values for  $\kappa/\nu$  respective to the fixed intrinsic viscosities chosen from literature were:  $\kappa/\nu = 0.31$ , using  $[\eta]_{\text{Monkos}}$ ; and  $\kappa/\nu = 0.42$ , using  $[\eta]_{\text{Tanford}}$ . These values were comparable to values reported for other globular proteins, such as IgG ( $\kappa/\nu = 0.37$  to 0.49) and hemoglobin ( $\kappa/\nu = 0.40$ ).<sup>12,18,35</sup>

The Ross–Minton model was fitted to the data allowing free parameters. The best fit computed was using experimental

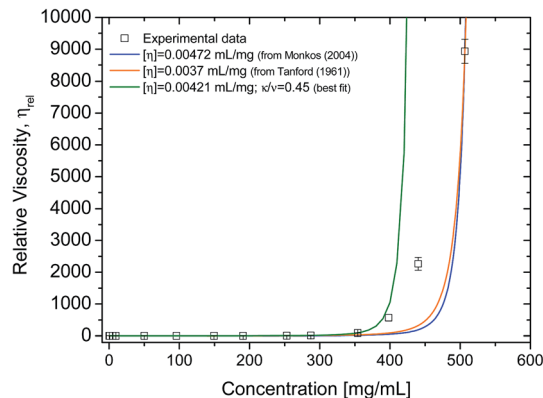


Fig. 6 Experimental cone-and-plate rheometry data (squares) fitted to Ross–Minton's equation (eqn (2)). Relative viscosity was obtained by dividing each of the sample's high shear viscosity ( $\sim 1000$  s<sup>-1</sup>) by the averaged buffer viscosity  $1.038 \pm 0.013$  mPa s. Fits were calculated by fixing  $[\eta]$  and leaving the parameter  $\kappa/\nu$  free and are as follows: blue line,  $[\eta] = 4.72 \times 10^{-3}$  mL mg<sup>-1</sup> (from ref. 3),  $\kappa/\nu = 0.31 \pm 6.6 \times 10^{-4}$ ,  $r^2 = 0.95$ ; orange line,  $[\eta] = 0.0037$  mL mg<sup>-1</sup> (from ref. 31),  $\kappa/\nu = 0.42 \pm 6.9 \times 10^{-4}$ ,  $r^2 = 0.94$ . Green line represents best fit of the same equation to experimental data using free parameters. Fit was calculated leaving both  $[\eta]$  and  $\kappa/\nu$  free:  $[\eta] = 4.21 \times 10^{-3} \pm 1.5 \times 10^{-4}$ ,  $\kappa/\nu = 0.45 \pm 0.024$ ;  $r^2 = 0.999$  and  $\chi^2 = 0.40$ . Experimental data used for this fit were only up to 350 mg mL<sup>-1</sup>.

data up to  $\sim 350$  mg mL<sup>-1</sup> (Fig. 6 – green line). Both the  $[\eta]$  ( $4.21 \times 10^{-3}$  mL mg<sup>-1</sup>) and  $\kappa/\nu$  (0.45) values were in agreement to the values reported in literature.<sup>8,15,20</sup> This fitted intrinsic viscosity value was similar to the intrinsic viscosity value calculated with triple detection HPSEC for the monomer peak of rAlbumin (Table 1). However, the Ross–Minton model did not predict solution viscosity for the highest concentrations ( $\geq 350$  mg mL<sup>-1</sup>).

The rheology data was fitted to the other hard-sphere model, the Krieger–Dougherty equation (eqn (3)). First, the intrinsic viscosity ( $[\eta]$ ) was fixed to 2.5, defined for spheres, and setting the maximum packing fraction ( $\phi_{\text{max}}$ ) to 0.64. Then, the data was fitted defining the maximum packing fraction to 0.71, while still assuming the protein species were spherical ( $[\eta] = 2.5$ ). In both cases, fixing intrinsic viscosity to 2.5 and  $\phi_{\text{max}}$  could only predict the data up to 100 mg mL<sup>-1</sup>, which is in agreement with the literature<sup>7</sup> (Fig. 7A – orange and magenta lines).

Conversion of weight/volume concentration to volume fraction was calculated *via* the polymer chemistry equation for volume fraction ( $\phi = N_A V c / MW_h$ ), taking into account the hydrated molecular weight of the protein –  $MW_h$  (eqn (10)). The hydrated protein molecular weight was calculated from  $MW_h = MW_p(1 + \delta)$ , where  $MW_p$  is the molecular weight of the protein and  $\delta$  is the amount of water associated with the macromolecule in g g<sup>-1</sup>.<sup>8,15</sup>

$$\phi = \frac{c}{MW_h} \left( N_A V + \frac{MW_p \delta}{\rho} \right) \quad (10)$$

where  $c$  is the concentration in mg mL<sup>-1</sup>,  $N_A$  is Avogadro's number,  $V$  is the protein's hydrodynamic volume (113.4 nm<sup>3</sup>), and  $\rho$  is the density of water at 20 °C ( $998.2 \times 10^3$  mg mL<sup>-1</sup>) and  $\delta = 0.379$ .<sup>8</sup>

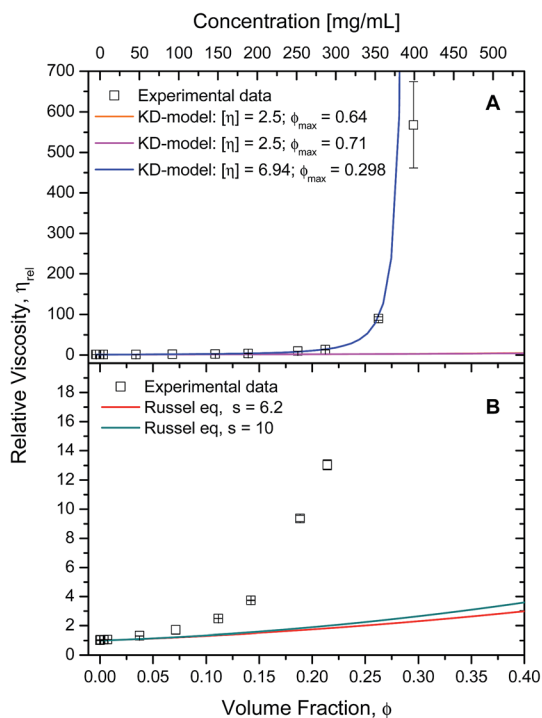


Fig. 7 A) Experimental cone-and-plate rheometry data (squares) plotted against expected data (lines) from Krieger–Dougherty's equation (eqn (3)) with fixed parameters. Relative viscosity was calculated by dividing each sample's ( $\eta$  (1000 s<sup>-1</sup>)) by the buffer's viscosity ( $\eta_0 = 1.038 \pm 0.013$  mPa s). For both lines,  $[\eta]$  was fixed to 2.5, but different  $\phi_{max}$  were used: 0.64 (orange); 0.71 (magenta). See text for more details. Data was fitted to Krieger–Dougherty's equation using free parameters (blue). Computed parameters were  $[\eta] = 6.9 \pm 0.14$ ,  $\phi_{max} = 0.30 \pm 0.0025$ , with  $r^2 = 0.999$  and  $\chi^2 = 0.26$ . Experimental data used for was up to 350 mg mL<sup>-1</sup>. (B) Experimental cone-and-plate rheometry data (squares) plotted against expected data (lines) from Russel's equation (eqn (4)) using fixed parameters. For both lines,  $[\eta]$  was fixed to 2.5, but  $s$  was: 6.2 (red line); 10 (green line).

The data was fitted to this model with free parameters, allowing a prediction of viscosity applied to non-spherical particles (Fig. 7A – blue line). The parameters which were best fits using data up to 350 mg mL<sup>-1</sup>, were  $[\eta] = 6.94 \pm 0.14$  and  $\phi_{max} = 0.298 \pm 0.002$  (with  $r^2 = 0.9996$  and  $\chi^2 = 0.26$ ). In this case, the fitted intrinsic viscosity showed a higher value than that corresponding to spheres, indicating that particle aspect ratio had increased and the  $\phi_{max}$  decreased respectively. These values suggest good physical significance, since their product is still within their usual range  $1.4 < [\eta]/\phi_{max} < 4$ .<sup>43</sup> The fitted intrinsic viscosity value of  $\sim 6.9$  agreed with the reported aspect ratio of albumin, known to be a prolate ellipsoid.<sup>8,15,40</sup> Altogether, these observations along with those previously made from the Ross–Minton model, point to a difficulty in prediction of solution viscosity of concentrations  $> 350$  mg mL<sup>-1</sup> (see Fig. 6 (green line) and 7A (blue line)).

The Russel–Saville–Schowalter equation<sup>4</sup> (eqn (4)), was used to fit our data since it takes into account the interparticle interaction. To fit the data to this model,  $s$ , the term which is defined by the effective distance between particles, was initially chosen to be equal to 6.2, as per Batchelor's proposal applied to

repulsive hard spheres.<sup>4</sup> However, Sharma *et al.*<sup>7</sup> showed that the data of concentrated BSA solutions up to 250 mg mL<sup>-1</sup> could fit with this model (with data up to  $\sim 250$  mg mL<sup>-1</sup>) using a value  $s = 10$ . The authors suggested that this value would correspond to an interaction potential corresponding to a  $d_{eff} = 2.5a$ , reflecting BSA's repulsive net negative charge in a saline buffer at pH  $\sim 7.10$ . The comparability between rAlbumin (or HSA) and BSA can be made since these two albumin variants share  $>75\%$  of their primary structure and many physical properties (*e.g.* surface hydrophobicity), having however, slight differences with regards to its thermal stability, electrophoretic behaviour and binding properties.<sup>44,45</sup>

This model could not predict the viscosity of our experimental data at concentrations higher than  $\sim 150$  mg mL<sup>-1</sup> ( $\phi = 0.11$ ), even when fixing  $s = 10$  (Fig. 7B). Since this model fixes the intrinsic viscosity at 2.5 for hard spheres, while it has been previously discussed that rAlbumin (and BSA) are not spherical but prolate ellipsoids, it may well not be the most appropriate albeit the only equation that includes surface charge as determinant to the viscosity of globular protein solutions.

The rheology data was further analysed using the generalised equations of Minton and Krieger–Dougherty for protein viscosity (eqn (7) and (8), respectively), which account for the presence of multiple species of protein in solution. By fitting these two generalised models to the experimental rheology data, it was found that the best fits would be achieved if the concentration range would not include either the last three (for eqn (8)) or two data points (for eqn (7)) (Fig. 8). The fitted weight-averaged intrinsic viscosity and  $w^*$  values suggest conformity between both generalised models. By using these generalised models it is still not possible to predict the higher concentrations above  $\sim 350$  mg mL<sup>-1</sup>. When fitting the experimental data using all the data points available, the fitted parameters usually presented poor statistical correlations

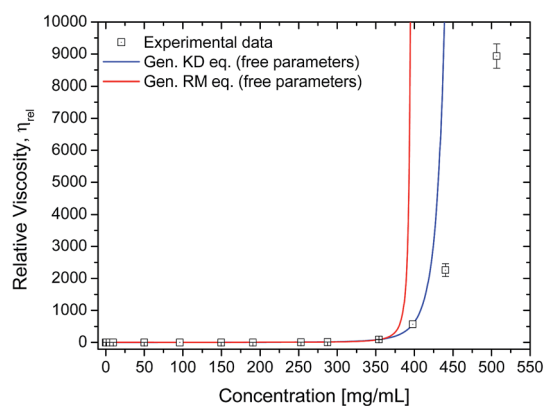


Fig. 8 Experimental data fitted to the generalised Krieger–Dougherty equation (eqn (8); blue line). Fitting parameters were  $[\eta]_w = 0.00517 \pm 1.1 \times 10^{-4}$  mL mg<sup>-1</sup>,  $w^* = 399 \pm 3.4$  mg mL<sup>-1</sup>, with  $r^2 = 0.999$  and  $\chi^2 = 0.26$ . Data used was up to 350 mg mL<sup>-1</sup>. Experimental data fitted to the generalised Ross–Minton equation (eqn (7), red line). Fitting parameters were  $[\eta]_w = 0.00479 \pm 4.0 \times 10^{-5}$  mL mg<sup>-1</sup>,  $w^* = 569 \pm 2.2$  mg mL<sup>-1</sup>, with  $r^2 = 1.0$  and  $\chi^2 = 0.91$ . Data used was up to 400 mg mL<sup>-1</sup>. For both plots, relative viscosity was calculated by dividing the sample's  $\eta$  (1000 s<sup>-1</sup>) by the buffer's viscosity (1.038  $\pm$  0.013 mPa s).



( $r^2 < 0.9$ ,  $\chi^2 \gg 1$ ) as well as higher values for  $[\eta]_w$  with no physical significance.

In the study by Galush *et al.*,<sup>26</sup> the protein mixtures were always prepared to a known total weight/volume concentration and known weight fractions of each of the proteins in the mixture. In our case, the presented HPSEC results (Fig. 2B) showed that the monomer, dimer and trimer composition was changing with sample concentration. Therefore, a weight-averaged intrinsic viscosity was calculated per sample (eqn (9)), instead of being assumed to remain constant (Table 2), using the data obtained by triple detection HPSEC (Table 1). The weight-averaged intrinsic viscosity values were slightly affected.

Using the calculated weight-averaged intrinsic viscosity, and assuming the different  $w^*$  values based on the fitted parameters obtained above, the viscosities were computed for the studied concentrations (Fig. 9A and B) for both generalised models. When choosing  $w^*$  of higher values (derived from fits using all data points), the viscosities were typically underestimated. On the other hand, using  $w^*$  values that were derived from the best fits, 569 mg mL<sup>-1</sup> for the generalised Ross–Minton model (eqn (7)), or 399 mg mL<sup>-1</sup> for the generalised Krieger–Dougherty model (eqn (8)), the viscosities were correctly predicted for the higher concentrations up to, and including, 450 mg mL<sup>-1</sup> and 350 mg mL<sup>-1</sup>, respectively.

## Discussion

The biophysical characterisation reported here aimed at providing a clear characterisation of the rheological behaviour, and the protein species content, of dilute to highly concentrated solutions of rAlbumin. From the steady shear rheology of these solutions, it was concluded that they showed a Newtonian-like behaviour. This is in clear contrast to previous studies of the rheology of globular proteins<sup>7,33,34,46</sup> where an apparent yield-behaviour has been reported, particularly at lower shear rates (<10 s<sup>-1</sup>). The reason for this purely viscous Newtonian-like behaviour is likely due to the presence of polysorbate-80, a well-known surfactant used in biopharmaceutical formulations. This is proposed to negate the effect on rheological properties of surface tension that can occur due to formation of

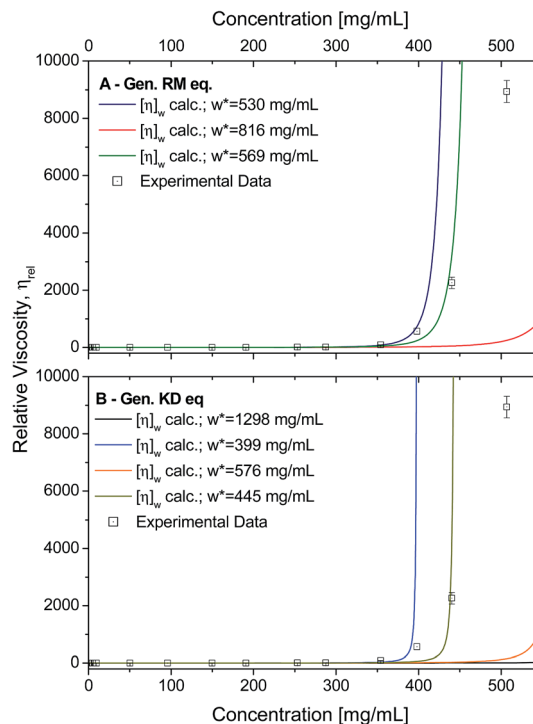


Fig. 9 A) Experimental data (squares) plotted against the calculated viscosities (lines) based on the generalised Ross–Minton equation (eqn (7)). Data was calculated when fixing the  $w^*$  to 530 mg mL<sup>-1</sup> (blue), 816 mg mL<sup>-1</sup> (red) and 568 mg mL<sup>-1</sup> (green). Fitted  $w^*$  values used were from best fits to eqn (7). (B) Experimental data (squares) plotted against the calculated viscosities (lines) based on the generalised Krieger–Dougherty equation (eqn (8)). Data calculated when fixing the  $w^*$  to 1298 mg mL<sup>-1</sup> (black), 399 mg mL<sup>-1</sup> (blue), 576 mg mL<sup>-1</sup> (orange), and 445 mg mL<sup>-1</sup> (light green). Fitted  $w^*$  values used are from best fits to eqn (8). For both plots, expected viscosities were calculating using  $[\eta]_w$  calculated in Table 2.

a protein film at the air–water interface.<sup>7</sup> Similar rheological behaviour has been reported for globular protein solutions in a buffer also containing a polysorbate surfactant.<sup>47,48</sup>

Fig. 2A clearly shows the viscosity increase with protein concentration. From the data in the figure, it is clear that a larger increase in viscosity occurred between concentrations

Table 2 Table with calculated  $[\eta]_w$  for rAlbumin solutions based on the experimental HPSEC triple detection data.  $[\eta]_1$  and  $[\eta]_2$  correspond to the average experimental intrinsic viscosity for monomer and dimer, respectively.  $f_1$  and  $f_2$  correspond to the fraction of relative peak area for monomer and dimer, respectively

Sample concentration (mg mL <sup>-1</sup> )	Monomer			Dimer			
	$f_1$ , peak area fraction	$w_1$ , mass fraction	$[\eta]_1 \times w_1$ ( $[\eta]_1 = 0.00409$ mL mg <sup>-1</sup> )	$f_1$ , peak area fraction	$w_1$ , mass fraction	$[\eta]_1 \times w_1$ ( $[\eta]_1 = 0.00471$ mL mg <sup>-1</sup> )	$[\eta]_w$
50.2	0.961	48.24	0.197	0.039	1.96	0.009	0.00411
96.0	0.960	92.16	0.377	0.040	3.84	0.018	0.00411
190.8	0.957	182.60	0.747	0.043	8.20	0.039	0.00412
253.1	0.957	242.22	0.991	0.043	10.88	0.051	0.00412
354.2	0.947	335.43	1.372	0.053	18.77	0.088	0.00412
398.0	0.945	376.11	1.538	0.055	21.89	0.103	0.00412
440.2	0.943	415.11	1.698	0.057	25.09	0.118	0.00413
506.8	0.939	475.89	1.946	0.061	30.91	0.146	0.00413

$\sim 250$  and  $\sim 500$   $\text{mg mL}^{-1}$ . The  $\sim 500$   $\text{mg mL}^{-1}$  sample reached a high shear rate viscosity of  $\sim 10\,000$  times larger than that of water ( $1.0016$   $\text{mPa s}$  at  $20$   $^{\circ}\text{C}$ , as defined by NIST). Although biopharmaceutical formulations are not typically formulated at more than  $200$   $\text{mg mL}^{-1}$ , the literature has discussed similar increases of viscosity.<sup>14,26,35</sup> Therefore, analysing the viscosity increase with concentration of rAlbumin solutions as a biopharmaceutical formulation model will help understand what factors govern this exponential rise in viscosity.

To correlate this increase in viscosity with the increase in protein concentration and its level of aggregation, further characterisation with HPSEC was needed. From Fig. 2B it is clear that there is an increase in dimer and trimer content for samples  $>250$   $\text{mg mL}^{-1}$ .

Triple-detection HPSEC allowed determination of the intrinsic viscosity and MW of each protein species detected in the conditions used here. Experimentally calculated molecular weight values for monomers and dimers agreed well with the values reported in literature for human serum and bovine serum albumin.<sup>36</sup> The values for intrinsic viscosity detected were however, quantitatively different to those in the literature, possibly due to differences in experimental conditions (*e.g.* temperature, mobile phase buffer and flow rate), which can affect the working conditions of the differential viscometer. However, our results for intrinsic viscosities were still statistically different ( $p < 0.05$ , one-way ANOVA) between monomer and dimer at every concentration studied. No variation with concentration was observed for the intrinsic viscosity values within specific molecular weight ranges.

The results obtained by DLS were similar to those described in literature<sup>40</sup> – only one peak was detected, with radii between  $3.8$ – $4.5$   $\text{nm}$  corresponding to the hydrodynamic radius of monomeric recombinant human albumin (Fig. 3). The hydrodynamic size distribution by volume showed a slight skew towards monomer size. This reflects the higher relative contribution of monomer in comparison to low relative quantity of dimers and trimers in solution. Data from microfluidic SDS-PAGE (Fig. SI-3†) confirmed the presence of monomers and dimers in the diluted solutions of samples from  $200$ – $500$   $\text{mg mL}^{-1}$ , and that no other higher molecular weight aggregates were present. This information was in agreement with our data from HPSEC characterisation.

Finally, the rheology results reported in Fig. 4 and 5 (recorded with mVROC) show that the rheology data of rAlbumin solutions recorded with a cone and plate rheometer, were free from surface-tension effects. When, samples were diluted with surfactant-free buffer it was clear that there were differences in the measured viscosities at high shear, compared to formulated protein solution. These differences are proposed to be related to the lower concentration of polysorbate-80 present in the  $5$  and  $10$   $\text{mg mL}^{-1}$  samples, and to some extent those at  $50$   $\text{mg mL}^{-1}$ . Polysorbate-80 is present in the formulation to prevent the macromolecule reaching the air/water and solid/water interface.<sup>27</sup> In these samples, as the surfactant was diluted during sample preparation to below its effective concentration, it likely ceased to be sufficient in preventing the protein from reaching the air–water interface present when using the cone–plate

geometry. As mentioned before, such surface tension effects have been proposed to influence torque measurements at low shear rates, leading to an apparent yield-behaviour observed as a pronounced increase in the slope of the viscosity function,<sup>7</sup> where the sample is no longer Newtonian. Other authors also observed similar differences when adding surfactants to globular protein solutions.<sup>47,48</sup> By studying the rheology of protein samples prepared in surfactant-containing buffer, it is proposed that the values of viscosity and shear stress measured and are similar to a measurement performed with an air–water interface-free instrumentation, such as the mVROC.

The results discussed so far showed that the rAlbumin solutions studied were constituted mainly of monomeric species with a small percentage of dimers and trimers, which increases, at the expense of monomers present in solution, when the solution is concentrated  $>250$   $\text{mg mL}^{-1}$ . Since this was also the concentration at which an increase in solution viscosity was noticed, it was important to analyse our rheology data with models that should predict the increase of viscosity with concentration.

In summary, our analysis suggested that concentrations above  $\sim 350$   $\text{mg mL}^{-1}$  have a solution viscosity that depends on factors other than those taken into account by the models explored here. These models have been developed based on their application to low concentrations of particle suspensions, where each particle would be far apart from another enough to not influence its flow.<sup>15</sup> Therefore, it is not surprising that these equations always apply well to lower concentrations of albumin.

Although the models presented here are based on hard quasi-spherical repulsive particles and their excluded volume, the predicted data typically suggest that a maximum packing fraction of rAlbumin (based on the best fits) will always be lower than the highest concentrations achieved experimentally ( $\sim 450$ – $500$   $\text{mg mL}^{-1}$ ). In addition, viscosity prediction, according to pure hard-sphere particle models, clearly underestimates the viscosity values for concentrations higher than  $\sim 100$ – $150$   $\text{mg mL}^{-1}$ .

One possible suggestion to explain such deviation from predictions at high concentration is that the maximum packing concentration could be dependent on solution composition *e.g.* the relative quantity of monomers and oligomeric species such as dimers and trimers. It is known that suspensions composed of binary sized spherical particles yield a maximum packing fraction approximately larger than the random close packing for a homogenous suspension.<sup>5,23–25</sup> However, albumin is a prolate ellipsoid that has been shown to influence the maximum packing fraction. It has been predicted that for globular protein solutions up to approximately  $250$   $\text{mg mL}^{-1}$  with the protein having a  $5 : 1$  aspect ratio, the increase of jamming limit would not be significant.<sup>14</sup> The models employed so far assume that associative species remain with the same globular shape, which is clearly not the case.

Apart from shape, it is unlikely that rAlbumin could resemble a hard particle, as its homologue HSA has been reported to exhibit a drop in intrinsic viscosity with temperature increase,<sup>8</sup> and its mammalian variant BSA has been shown to have an intrinsic viscosity which is pH-dependent.<sup>49</sup> These

studies, along with others from protein hydrodynamic analysis,<sup>44,50</sup> point towards the influence of protein conformation in viscosity studies, *via* a change in intrinsic viscosity depending on the solution conditions. Therefore, as the protein is further concentrated, changes in protein conformation could be a factor to account for the slow increase of viscosity compared to hard sphere model predictions. In addition, this slow increase could also be due to the repulsive nature of inter-protein interactions, which is a phenomenon that has been observed for sterically stabilised colloids.<sup>22</sup>

The deviation from models seen at higher concentrations ( $\geq 350 \text{ mg mL}^{-1}$ ) could be related to a glass transition similar to that which occurs with colloidal hard spheres. In this case, accounting for repulsive excluded volume, suspensions are expected to approach a glass transition at volume fractions  $\phi \approx 0.58$  before approaching the random close packing fraction ( $\phi = 0.64$ ).<sup>22</sup> When the concentration approaches a glassy state, the particle is caged by the presence of neighbouring particles, thus slowing down its flow and leading to increased viscosities. In the case of rAlbumin, an analogous glass transition behaviour could be taking place at the concentrations between  $\sim 400$  to  $\sim 500 \text{ mg mL}^{-1}$  based on similar results seen with highly concentrated solutions of BSA.<sup>51</sup> This would suggest that these concentrations are approaching the jamming limit but does not explain why viscosities cannot be predicted in conventional models. Finally, it is precisely the sample range between  $350 \text{ mg mL}^{-1}$  and  $500 \text{ mg mL}^{-1}$  that showed an increase in the relative quantity of dimers (with a respective decrease of monomers). Therefore, it does suggest that the change of composition and the increase of viscosity with increase of concentration are connected and needs to be addressed in these models.

## Conclusions

In this work a range of rAlbumin solutions, in a formulation buffer containing NaCl and a surfactant, were analysed for their rheological behaviour with the aim of understanding the effects of high concentration on solution viscosity. Rheological measurements showed that the solutions behaved as purely viscous fluids in the range of the applied shear rates. It was observed that as the protein concentration increased in solution, the samples presented an increase of viscosity. All samples showed the same oligomeric species were present in solution; monomers, dimers and trimers of rAlbumin. As concentration increased to  $\sim 500 \text{ mg mL}^{-1}$ , the relative quantity of dimers and trimers increased along with a corresponding decrease of monomer. By DLS and microfluidic SDS-PAGE analysis, the solutions showed no other signs of impurities such as other higher order aggregates or protein fragments. Throughout this study several experiments proved that concentrating the rAlbumin  $\geq 200 \text{ mg mL}^{-1}$  did not seem to have any other effect besides the increase of solution viscosity and the change in relative composition of protein species.

A comprehensive theoretical analysis of the rheological experimental data was performed using different models that are commonly applied to predict protein solution viscosity. The Ross–Minton and Krieger–Dougherty equations were

demonstrated to predict our experimental data up to  $350 \text{ mg mL}^{-1}$ . When considering the protein inter-distance and thus the effect of interaction potential upon viscosity, the solution viscosity couldn't be predicted for concentrations  $\geq 150 \text{ mg mL}^{-1}$ .

Generalised versions of the Ross–Minton and Krieger–Dougherty equations were also studied and the results showed that the former could successfully fit when using experimental data up to  $\sim 400 \text{ mg mL}^{-1}$  of rAlbumin. Although these models assume that the protein species are hard particles throughout all conditions observed, the equations account for multiple/oligomer species, which determines a weighted approach to intrinsic viscosity suggesting a variation in these species as protein concentration increases. The fact that our analysis produced better fits using these generalised equations further highlights the importance of considering the variation in composition within a protein solution, thus justifying the complete characterisation of oligomeric species present. It is important to note that no other analysis typically accounts for this variation using a sample composed of one protein only. We however suggest that other factors related to highly concentrated solutions may still also need to be considered, particularly since those concentrations not fitted were the most concentrated ( $>400 \text{ mg mL}^{-1}$ ), where crowding effects should be more accentuated.

In conclusion, the example of rAlbumin explored here highlights that knowledge of how the protein oligomeric species composition varies between samples of increasing concentration, is a key factor for predicting the viscosity of protein solutions. Application of this knowledge to liquid formulations of therapeutic macromolecules (such as mAbs) would be important to further understand their solution viscosities. However, in this case, protein structure could also play an important role, where protein–protein interactions between protein domains have been shown to influence solution viscosity.<sup>11,12</sup>

The relevance of this study to pharmaceutical sciences is that it ultimately shows the importance of better understanding the underlying factors leading to the high viscosity of highly concentrated biopharmaceutical liquid formulations. By using improved models, prediction of protein solution viscosity could eventually bring advantage to early phase development studies, and ultimately help develop better highly concentrated biopharmaceutical formulations, allowing painless sub-cutaneous administration to patients.

## Acknowledgements

A. D. G. is grateful for EPSRC and AstraZeneca for funding this work (Grant EP/D501849/1).

## References

- 1 S. J. Shire, Z. Shahrokh and J. Liu, *J. Pharm. Sci.*, 2004, **93**, 1390–1402.
- 2 J. Jezek, M. Rides, B. Derham, J. Moore, E. Cerasoli, R. Simler and B. Perez-Ramirez, *Adv. Drug Delivery Rev.*, 2011, **63**, 1107–1117.

- 3 I. M. Krieger and T. J. Dougherty, *Trans. Soc. Rheol.*, 1959, **III**, 137–152.
- 4 W. B. Russel, D. A. Saville and W. R. Schowalter, *Colloidal Dispersions*, 1st edn, 1989.
- 5 R. D. Sudduth, *J. Appl. Polym. Sci.*, 1993, **48**, 25–36.
- 6 B. Lonetti, E. Fratini, S. H. Chen and P. Baglioni, *Phys. Chem. Chem. Phys.*, 2004, **6**, 1388–1395.
- 7 V. Sharma, A. Jaishankar, Y. Wang and G. H. Mckinley, *Soft Matter*, 2010, **7**, 5150–5161.
- 8 K. Monkos, *Biochim. Biophys. Acta*, 2004, **1700**, 27–34.
- 9 B. A. Salinas, H. A. Sathish, S. M. Bishop, N. Harn, J. F. Carpenter and T. W. Randolph, *J. Pharm. Sci.*, 2009, **99**, 82–93.
- 10 S. Yadav, S. J. Shire and D. S. Kalonia, *Pharm. Res.*, 2011, **28**, 1973–1983.
- 11 J. Liu, M. D. H. Nguyen, J. D. Andya and S. J. Shire, *J. Pharm. Sci.*, 2005, **94**, 1928–1940.
- 12 S. Kanai, J. U. N. Liu, T. W. Patapoff and S. J. Shire, *J. Pharm. Sci.*, 2008, **97**, 4219–4227.
- 13 S. Yadav, A. Sreedhara, S. Kanai, J. Liu, S. Lien, H. Lowman, D. S. Kalonia and S. J. Shire, *Pharm. Res.*, 2011, **28**, 1750–1764.
- 14 A. P. Minton, *J. Phys. Chem. B*, 2012, **116**, 9310–9315.
- 15 C. Tanford, *Physical Chemistry of Macromolecules*, John Wiley & sons, Inc., 1st edn, 1961.
- 16 S. M. Loveday, L. K. Creamer, H. Singh and M. A. Rao, *J. Food Sci.*, 2007, **72**, R101–R107.
- 17 C. Tanford and J. G. Buzzell, *J. Phys. Chem.*, 1956, **60**, 225–231.
- 18 P. D. Ross and A. P. Minton, *Biochem. Biophys. Res. Commun.*, 1977, **76**, 971–976.
- 19 J. Lefevre, *Rheol. Acta*, 1982, **21**, 620–625.
- 20 S. Harding, *Prog. Biophys. Mol. Biol.*, 1997, **68**, 207–262.
- 21 M. Mooney, *J. Colloid Sci.*, 1951, **6**, 162–170.
- 22 J. Mewis and N. Wagner, *Colloidal Suspension Rheology*, Cambridge University Press, UK, 1st edn, 2012.
- 23 B. Dames, B. R. Morrison and N. Willenbacher, *Rheol. Acta*, 2001, **40**, 434–440.
- 24 R. D. Sudduth, *J. Appl. Polym. Sci.*, 1993, **48**, 37–55.
- 25 R. D. Sudduth, *J. Appl. Polym. Sci.*, 1993, **50**, 123–147.
- 26 W. J. Galush, L. A. N. N. Le and J. M. R. Moore, *J. Pharm. Sci.*, 2012, **101**, 1012–1020.
- 27 E. Tarelli, A. Mire-Sluis, H. A. Tivnann, B. Bolgiano, D. T. Crane, C. Gee, X. Lemercinier, M. L. Athayde, N. Sutcliffe, P. H. Corran and B. Rafferty, *Biologicals*, 1998, **26**, 331–346.
- 28 S. Curry, H. Mandelkow, P. Brick and N. Franks, *Nat. Struct. Biol.*, 1998, **5**, 827–835.
- 29 M. Dockal, D. C. Carter and F. Rüker, *J. Biol. Chem.*, 2000, **275**, 3042–3050.
- 30 C. J. Pipe, T. S. Majmudar and G. H. McKinley, *Rheol. Acta*, 2008, **47**, 621–642.
- 31 C. W. Macosko, *Rheology: principles, measurements, and applications*, VCH, New York, 1st edn, 1994.
- 32 H. Zhao, P. H. Brown and P. Schuck, *Biophys. J.*, 2011, **100**, 2309–2317.
- 33 S. Ikeda and K. Nishinari, *Biomacromolecules*, 2000, **1**, 757–763.
- 34 S. Ikeda and K. Nishinari, *Food Hydrocolloids*, 2001, **15**, 401–406.
- 35 S. Yadav, S. J. Shire, D. S. Kalonia and J. U. N. Liu, *J. Pharm. Sci.*, 2010, **99**, 1152–1168.
- 36 P. Clarke and J.-L. Brousseau, Pharmaceutical Online, <http://www.malvern.com/en/support/resource-center/articles/AR100203AdvancedSECPPharmaceuticalDevelopment.aspx> accessed May 2013.
- 37 J. P. Gabrielson, M. L. Brader, A. H. Pekar, K. B. Mathis, G. Winter, J. F. Carpenter and T. W. Randolph, *J. Pharm. Sci.*, 2007, **96**, 268–279.
- 38 T. Arakawa, D. Ejima, T. Li and J. S. Philo, *J. Pharm. Sci.*, 2010, **99**, 1674–1692.
- 39 S. J. Burton, A. V. Quirk and P. C. Wood, *Eur. J. Biochem.*, 1989, **179**, 379–387.
- 40 B. Jachimska, M. Wasilewska and Z. Adamczyk, *Langmuir*, 2008, **24**, 6866–6872.
- 41 J. L. Richards, *J. Chem. Educ.*, 1993, **70**, 685.
- 42 F. Soetewey, M. Rosseneu-motreff, R. Lamote and H. Peeters, *J. Biochem.*, 1972, **71**, 705–710.
- 43 R. G. Larson, *The Structure and Rheology of Complex Fluids*, Oxford University Press, UK, 1st edn, 1999.
- 44 L. R. S. Barbosa, M. G. Ortore, F. Spinozzi, P. Mariani, S. Bernstorff and R. Itri, *Biophys. J.*, 2010, **98**, 147–157.
- 45 A. Michnik, K. Michalik, A. Kluczevska and Z. Drzazga, *J. Therm. Anal. Calorim.*, 2006, **84**, 113–117.
- 46 S. Ikeda and K. Nishinari, *Int. J. Biol. Macromol.*, 2001, **28**, 315–320.
- 47 A. Jaishankar, V. Sharma and G. H. Mckinley, *Soft Matter*, 2011, **7**, 7623–7634.
- 48 T. W. Patapoff and O. Esue, *Pharm. Dev. Technol.*, 2009, **14**, 659–664.
- 49 P. S. Sarangapani, S. D. Hudson, K. B. Migler and J. A. Pathak, *Biophys. J.*, 2013, **105**, 2418–2426.
- 50 N. El Kadi, N. Taulier, J. Y. Le Huérou, M. Gindre, W. Urbach, I. Nwigwe, P. C. Kahn and M. Waks, *Biophys. J.*, 2006, **91**, 3397–3404.
- 51 G. J. Brownsey, T. R. Noel, R. Parker and S. G. Ring, *Biophys. J.*, 2003, **85**, 3943–3950.